

Morphological and biochemical changes in *Pseudomonas fluorescens* biofilms induced by sub-inhibitory exposure to antimicrobial agents

James J. Dynes, John R. Lawrence, Darren R. Korber, George D.W. Swerhone, Gary G. Leppard, and Adam P. Hitchcock

Abstract: Confocal laser scanning microscopy (CLSM) and scanning transmission X-ray microscopy (STXM) were used to examine the morphological and biochemical changes in *Pseudomonas fluorescens* biofilms grown in the presence of subinhibitory concentrations of 4 antimicrobial agents: triclosan, benzalkonium chloride, chlorhexidine dihydrochloride, and trisodium phosphate. CLSM analyses using the stains SYTO9 and propidium iodide indicated that the antimicrobial agents affected cell membrane integrity and cellular density to differing degrees. However, fluorescein diacetate assays and plate counts demonstrated that the cells remained metabolically active. Fluorescent lectin binding assays showed that changes in the arrangement and composition of the exopolymer matrix of the biofilms also occurred and that these changes depended on the antimicrobial agent. Detailed single cell analyses using STXM provided evidence that the cell morphology, and the spatial distribution and relative amounts of protein, lipids and polysaccharides in the biofilms and within the cells were different for each antimicrobial. The distribution of chlorhexidine in the biofilm, determined from its distinct spectral signature, was localized mainly inside the bacterial cells. Each antimicrobial agent elicited a unique response; *P. fluorescens* cells and biofilms changed their morphology and architecture, as well as the distribution and abundance of bio-macromolecules, in particular the exopolymer matrix. *Pseudomonas fluorescens* also exhibited adaptation to benzalkonium chloride at 10 µg/mL. Our observations point to the importance of changes in the quantity and chemistry of the exopolymeric matrix in the response to antimicrobial agents and suggest their importance as targets for control.

Key words: NEXAFS, STXM, biofilm, antimicrobial, CLSM.

Résumé : La microscopie de balayage confocal de laser (MBCL ou CLSM) et la microscopie de balayage par transmission de rayons X (MBTX ou STXM) ont été utilisées pour examiner les changements morphologiques et biochimiques des biofilms de *Pseudomonas fluorescens* cultivés en présence de concentrations sub-inhibitrices de 4 agents antimicrobiens : le triclosane, le chlorure de benzalkonium, le dihydrochlorure de chlorhexidine et le phosphate trisodique. Les analyses en CLSM réalisées à l'aide du colorant SYTO9 et de l'iodure de propidium ont indiqué que les agents antimicrobiens affectaient l'intégrité de la membrane cellulaire et la densité cellulaire à différents degrés. Cependant, les essais réalisés avec le diacétate de fluorescéine et la numération en boîte ont démontré que les cellules demeuraient métaboliquement actives. Des essais de liaison de lectines fluorescentes ont montré que des changements dans l'arrangement et la composition de la matrice d'exopolymères des biofilms survenaient également, et que ces changements dépendaient de l'agent antimicrobien. Des analyses détaillées réalisées sur des cellules isolées par STXM ont prouvé que la morphologie cellulaire ainsi que la distribution spatiale et les quantités relatives des protéines, des lipides et des polysaccharides des biofilms et des cellules différaient en fonction des agents antimicrobiens. La distribution de la chlorhexidine dans les biofilms, déterminée par sa signature spectrale distincte, était localisée principalement à l'intérieur des cellules bactériennes. Chaque agent antimicrobien induisait une réponse unique; les cellules et les biofilms de *P. fluorescens* changeaient de morphologie et d'architecture, et la distribution et l'abondance des biomacromolécules étaient aussi modifiées, notamment dans la matrice d'exopolymères. *Pseudomonas fluorescens* montrait aussi une adaptation au chlorure de benzalkonium à 10 µg/mL. Nos observations soulignent l'importance des changements dans la quantité et la chimie de la matrice d'exopolymères en réponse aux agents antimicrobiens et suggèrent que ces changements constituent des cibles de contrôle importantes.

Mots-clés : NEXAFS, STXM, biofilm, antimicrobien, CLSM.

[Traduit par la Rédaction]

Received 17 September 2008. Accepted 1 October 2008. Published on the NRC Research Press Web site at cjm.nrc.ca on 5 March 2009.

J.J. Dynes and A.P. Hitchcock. Brockhouse Institute for Materials Research, McMaster University, Hamilton, ON L8S 4M1, Canada.

J.R. Lawrence¹ and G.D. Swerhone. Environment Canada, 11 Innovation Blvd, Saskatoon, SK S7N 3H5, Canada.

D.R. Korber. Food and Bioproduct Sciences, University of Saskatchewan, Saskatoon, SK S7N 5A8, Canada.

G.G. Leppard. Environment Canada, P.O. Box 5050, Burlington, ON L7R 4A6, Canada.

¹Corresponding author (e-mail: john.lawrence@ec.gc.ca).

Introduction

Biofilms are communities of microorganisms surrounded by extracellular polymeric substances (EPS) that can grow on all types of hydrated surfaces, including foodstuffs, food processing equipment, and medical devices. In the food industry, biofilm formation can lead to food contamination, reduced shelf life of food products, and transmission of disease; accordingly, a variety of antimicrobial agents are commonly employed to control biofilm formation. While usually effective, microorganisms periodically develop resistance to antimicrobial agents, something that has become an ongoing challenge to the food industry. Countermeasures to antimicrobial resistance could be developed from an improved understanding of how the morphology and biochemistry of biofilms are affected by antimicrobial agents.

Differences in biofilm response to antimicrobial agents may be ascribed to the variation in the structure and chemical composition of the antimicrobial agents, to the genetically determined morphology and biochemistry of the biofilm, and to how the antimicrobial agent interacts with the biofilm (Lindsay and Von Holy 2006). The minimum inhibitory concentration (MIC) is defined as the lowest concentration of a given antimicrobial agent sufficient to inhibit the growth of a given species of microorganism. Sub-inhibitory antimicrobial concentrations are those concentrations below the MIC (sub-MIC) that inhibit normal cellular functions without causing death. Examination of how sub-MIC impact different organisms has proven to be a useful approach to investigate antimicrobial resistance mechanisms (López-Diez et al. 2005; Okamoto et al. 2002; Wojnicz and Jankowski 2007; Majtán et al. 2008).

Biofilm-based resistance may be evaluated effectively using direct visualization and analysis techniques (Lawrence et al. 2003, 2007a; Neu and Lawrence 2005; Mangalappallillathu and Korber 2006). Confocal laser scanning microscopy (CLSM) has been used to assess cell viability, cell morphology, biofilm structure, and the form and composition of the exopolymer matrix of the biofilm (Korber et al. 1994; Lawrence et al. 2007a, b; Neu et al. 2001). Scanning transmission X-ray microscopy (STXM) has been used to quantitatively map the major classes of biomacromolecules (e.g., protein, lipids, and polysaccharides), and chlorhexidine in biofilms at a spatial resolution of <50 nm in hydrated biofilms (Hitchcock et al. 2002; Lawrence et al. 2003; Dynes et al. 2006b).

Pseudomonas fluorescens is ubiquitous in nature and considered to be an important food spoilage organism associated with fresh produce (Hadjok et al. 2008) and meats (Ouattara et al. 1997). *Pseudomonas fluorescens* CC-840406-E is an environmental isolate that has been extensively studied in our laboratory (Caldwell and Lawrence 1986; Korber et al. 1989). Its biofilm formation and growth characteristics are well known. Antimicrobial agents such as chlorhexidine (CHX), triclosan (TCS), trisodium phosphate (TSP), and benzalkonium chloride (BAC) are commonly used in the food and personal care product industries. Comparative studies provide an opportunity to examine how antimicrobial agents, with different modes of action, influence the properties of bacterial cells and biofilms. Accordingly, a combination of CLSM and STXM was used to characterize

the biochemical and morphological changes that occur in *P. fluorescens* in response to sub-MIC of TCS, chlorhexidine dihydrochloride, BAC, and TSP. Direct observation at the microscale is anticipated to allow detection of changes in the bacteria and biofilms that may point to alternate adaptation/resistance mechanisms and possible targets for control which have been under-studied.

Materials and methods

Sample preparation

Pseudomonas fluorescens strain CC-840406-E was used for all experiments. The details of its isolation and surface colonizing characteristics have been described previously (Caldwell and Lawrence 1986; Korber et al. 1989). Cultures were stored at -80°C in sterile 2 mL cryogenic vials (Corning Glass Works, Corning, New York) containing 3 mm borosilicate glass beads (Kirsop and Snell 1984). Biofilms were prepared by inoculating continuous-flow slide culture chambers (flow cells) with a 1-mL suspension of log-phase cells obtained from batch cultures grown in 50 mL of 10% trypticase soy broth (TSB) (3 g/L) on a gyratory shaker at $21^{\circ}\text{C} \pm 2^{\circ}\text{C}$. Flow cells (see CLSM and STXM design specification details below) were irrigated with minimal growth medium [3 mmol/L $\text{Na}_2\text{HPO}_4 \cdot 7\text{H}_2\text{O}$, 2 mmol/L KH_2PO_4 , 0.8 mmol/L $(\text{NH}_4)_2\text{SO}_4$, 0.4 mmol/L $\text{MgSO}_4 \cdot 7\text{H}_2\text{O}$, 0.02 mmol/L $\text{Ca}(\text{NO}_3)_2 \cdot 4\text{H}_2\text{O}$, and 0.8 $\mu\text{mol/L}$ FeSO_4] (Lawrence et al. 1991) containing 1 g/L of glucose at $21^{\circ}\text{C} \pm 2^{\circ}\text{C}$, at a laminar flow velocity using a peristaltic pump (Watson Marlow, Wilmington, Massachusetts). The CLSM flow cells were viewed after 24 or 96 h (see staining and lectin details below) and for the STXM experiments the silicon nitride window was removed from the flow cell after 24 h (see wet cell preparation details below). The CLSM experiments were repeated 3 times, on separate occasions, while the STXM experiments were repeated twice on separate occasions. The STXM flow cells were always run at the same time as the CLSM flow cells. Generally, 1 image sequence was selected per biofilm for detailed chemical analysis in the STXM studies, as time available on the beamline was limited. For the CLSM 3–7 areas in a biofilm were examined per CLSM experiment.

The biofilms were grown in the absence (control) and presence of selected antimicrobial agents: TCS (5-chloro-2-(2,4-dichlorophenoxy)phenol), BAC (alkylbenzyltrimethylammonium chloride), CHX (1,1'-hexamethylene bis[5-(*p*-chlorophenyl)biguanide]), and TSP. All chemicals were obtained from Sigma-Aldrich and were >95% pure.

The concentrations of the antimicrobial agents used in this study were 3, 10, 1, and 1000 $\mu\text{g/mL}$ for TCS, BAC, CHX, and TSP, respectively. For BAC, CHX, and TSP the concentrations were selected to be ~50% below the planktonic MIC (i.e., sub-MIC). The planktonic MIC values were determined by monitoring bacterial growth in a 10% TSB solution containing selected concentrations of each antimicrobial agent, by measuring the optical density at 600 nm (OD_{600}) (Cheung et al. 2007) at 20 min intervals over a 24 h period at $21^{\circ}\text{C} \pm 2^{\circ}\text{C}$. The MIC value was noted as the lowest antimicrobial concentration at which bacterial growth was not observed. For TCS, the *P. fluorescens* strain CC-840406-E was determined to be resistant at all concentrations includ-

ing saturation (~30 µg/mL). However, in the minimal growth media the solubility of TCS was about an order of magnitude less than that observed in the 10% TSB media, hence, the reason for using much less than 50% below the planktonic MIC as used for the other antimicrobial agents. The BAC was dissolved in water and filter sterilized through a 0.22 µm filter into the autoclaved minimal growth media, while the other antimicrobials were added as powders directly into the autoclaved minimal growth media. Microbial growth was never observed in the media reservoirs, confirming that the minimal growth media remained sterile after the addition of the antimicrobial agents and throughout the experiments.

An index of viable cells released from the biofilm was obtained by collecting the effluent from the CLSM chamber exit tubes of the 96-h biofilms in duplicate and spreading appropriate dilutions on 10% trypticase soy agar plates (Wolfaardt et al. 1994b). The number of colony forming units (CFU) per millilitre was determined after 24 h incubation of the agar plates at 21 °C ± 2 °C. The presence of only the *P. fluorescens* colonial morphotype also confirmed that no contamination of the apparatus occurred during the experiments.

Flow cell design specifications

The flow cells used for the CLSM experiments were constructed of polycarbonate and glass. Multiple 40 mm × 3 mm × 1 mm (length × width × depth) channels were milled into the polycarbonate, then covered with a No. 1 cover slip sealed in place with self-leveling RTV silicon adhesive (WPI, Sarasota, Florida), which allowed for microscopic examination of the biofilm growing on the cover slip (Wolfaardt et al. 1994a). Before inoculation, a 6% sodium hypochlorite solution was used to surface sterilize the CLSM flow cells for 1 h prior to rinsing with sterile water and medium.

For the STXM experiments, the biofilm was grown directly on silicon nitride membranes (Silson Ltd., Blisworth, United Kingdom) mounted in the flow cells, after which the silicon nitride membranes were removed from the flow cells and a wet cell constructed for analyses, as described previously (Dynes et al. 2006a, 2006b). STXM flow cells were constructed from 2 glass microscope slides separated by a gasket made from the silicon adhesive. In one slide, two 3 mm holes were drilled at each end and silicone tubing was glued to the holes using silicone adhesive to form inlet and outlet ports. The silicon nitride membrane was attached to the unmodified slide with a butterfly clamp made from cover slips fastened to the slide along 1 edge with silicone adhesive. This chamber design permitted easy removal of the delicate silicon nitride membrane. The STXM flow cell dimensions were 40 mm × 15 mm × 1 mm (length × width × depth). The STXM flow cells containing the silicon nitride membrane were autoclaved before inoculation. Because of the difference in cross-sectional areas the flow velocities were 0.01 (CLSM) and 0.04 cm/s (STXM). To check for possible flow velocity effects, the biofilms growing on the glass slides of the STXM chamber was compared with the CLSM experiments. The results (not shown) were not significantly different from the 24 h CLSM biofilms (Fig. 1).

Confocal laser scanning microscopy (CLSM) and probes

CLSM image sequences were collected using an MRC 1024 confocal laser scanning microscope (Zeiss, Jena, Germany) attached to a Microphot SA microscope (Nikon, Tokyo, Japan) equipped with a plan-apochromat, oil immersion 60×, 1.4 numerical aperture lens. To investigate membrane integrity, biofilm bacteria were stained simultaneously with SYTO9 and propidium iodide (PI) in situ (Invitrogen Molecular Probes, Eugene, Oregon). Fluorescence of SYTO9 and PI were recorded in the green (excitation/emission 488/522 nm) and red channels (excitation/emission 535/617 nm), respectively. Biofilm thickness and the cellular density were determined by image analysis of CLSM image sequences (Lawrence et al. 2007a). Comparison of the results was conducted with 1-way ANOVA using a commercial statistical software package (MiniTab, State College, Pennsylvania).

The fluor-conjugated lectins *Triticum vulgare* (specific for *N*-acetyl-glucosamine residues and oligomers) and *Vicia villosa* (specific for *N*-acetylgalactosamine) (Invitrogen Molecular Probes) were used to investigate changes in the form, arrangement, and composition of the EPS in the 96 h biofilms (Neu et al. 2001). The fluorescence from the lectin labels attached to *T. vulgare* and *V. villosa* was recorded in the red (excitation/emission 568/598 nm) and green (excitation/emission 488/522 nm) channels, respectively.

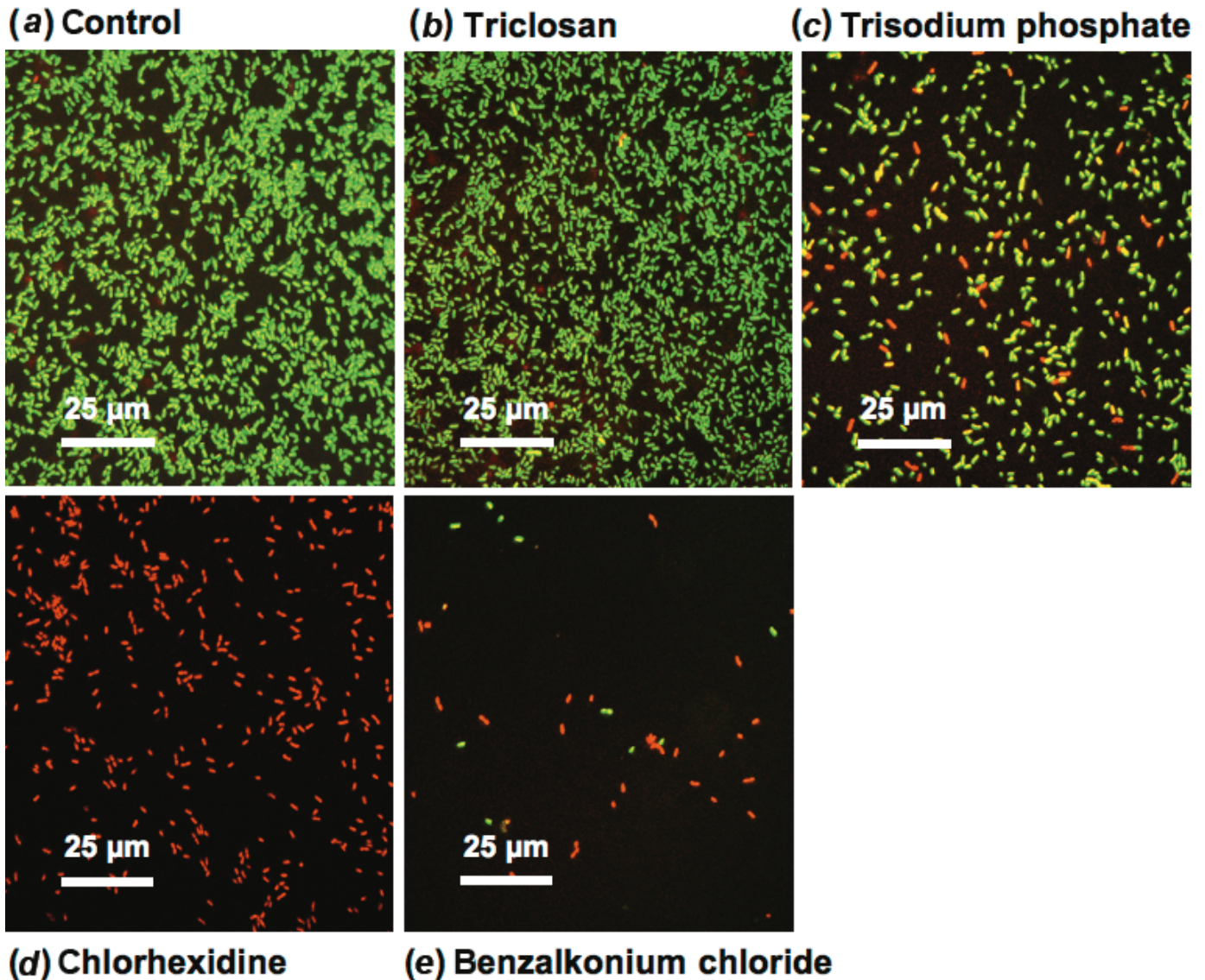
As an additional measure of cell viability, 5- and 6-carboxyfluorescein diacetate (FDA) was added to the 24 h biofilms (Breeuwer et al. 1996). Cells that are metabolically active can cleave the diacetate, allowing the released fluorescein (excitation/emission 492/517 nm) to fluoresce (recorded in the green channel).

Scanning transmission X-ray microscopy and data analysis

X-ray imaging and spectromicroscopy were carried out at the Advanced Light Source (Berkeley, California) using the STXM at beamline 5.3.2 (Kilcoyne et al. 2003; Warwick et al. 2002). STXM was used analytically by recording images at a sequence of energies (Jacobsen et al. 2000). Sequences of 80–100 images between 280 and 320 eV (C 1s, and K 2p regions) were recorded and converted to chemical component maps by fitting the optical density spectrum at each pixel to the spectra of the reference compounds (protein, lipid, polysaccharide, CO₃²⁻, K, and, where possible, the appropriate antimicrobial compound). The reference spectra of the biological components and chlorhexidine dihydrochloride have been presented elsewhere (Lawrence et al. 2003; Dynes et al. 2006b). The raw transmitted signals were converted to optical densities (absorbance) using incident flux signals measured through regions of the wet cell devoid of biofilm, to correct for the absorbance by the silicon nitride membranes and water, and to compensate for the spectral shape of the incident flux. The microscope energy scale was calibrated to an accuracy of ±0.05 eV using the Rydberg peaks of CO₂.

Quantitative component maps were derived for the major biomacromolecules (protein, lipids, and polysaccharides) and chlorhexidine by spectral fitting of C 1s image sequences measured between 280 and 320 eV using the singular value decomposition (SVD) procedure (Jacobsen et al.

Fig. 1. Confocal laser scanning microscopy images of 24 h *Pseudomonas fluorescens* biofilms grown in the presence and absence of antimicrobial agents. (a) Control, (b) triclosan (TCS), (c) trisodium phosphate (TSP), (d) chlorhexidine dihydrochloride (CHX), and (e) benzalkonium chloride (BAC). The biofilm was stained with SYTO9 (green) and propidium iodide (red).



2000; Koprinarov et al. 2002; Dynes et al. 2006a). Note that C 1s component maps for BAC and TCS could be derived when these antimicrobials were included in the fitting procedure; however, based on our methodology (Dynes et al. 2006a, 2006b), the C 1s near-edge X-ray absorption fine structure (NEXAFS) signals for BAC and TCS were not intense enough or sufficiently different to distinguish the TCS or BAC contributions from those of the biomacromolecular components of the biofilm with confidence. Hence, only the CHX component maps are discussed. The reference spectra, recorded from pure materials, were placed on absolute linear absorbance scales (OD for 1 nm) by matching them to the predicted response for the compound based on its elemental composition and density, using tabulated continuum absorption coefficients (Henke et al. 1993). The component concentration is reported as the thickness (in nm) at each pixel, which in turn depends on assumptions as to the effective density of each component. Where individual component

maps are given, the lower and upper limits of the gray scale are indicated. The reliability of the mapping for each component was evaluated using previously described methodology (Dynes et al. 2006a, 2006b), including examination of the residual image, examination of the fit of the spectrum to areas with the highest concentration identified by applying a grayscale threshold technique, and by exploring different reference compounds and combinations thereof. The relative amount of protein, lipid, and polysaccharide in the entire biofilm was calculated from the respective component maps by first integrating the thickness of these components over the regions they were located, and second, ratio-ing the amount for each species to the sum of the amounts of protein, lipid, and polysaccharide. Since the amount of antimicrobial agent (CHX, BAC, and TCS) in any sample was extremely small, these relative compositions did not depend on whether the antimicrobial agent was included in the fit or not. The uncertainty in the scales for the component maps is

Table 1. Minimum inhibitory concentrations (MIC) of planktonic *Pseudomonas fluorescens* cell cultures for specific antimicrobial agents, treatment concentrations, and the initial solution pH of the minimal growth media amended with antimicrobial agents.

Treatment	Minimum inhibitory concn. (MIC; $\mu\text{g/mL}$)	Treatment concn. ($\mu\text{g/mL}$)	Initial pH in minimum growth media
Control	NA	NA	6.9
Triclosan	Resistant	3 ^a	6.9
Benzalkonium chloride	20	10	7.1
Trisodium phosphate	2000	1000	11.0
Chlorhexidine dihydrochloride	2	1	6.9

Note: NA, not applicable.

^aMaximum concentration of TCS that dissolved in the minimum growth media.

estimated to be ~10% relative and 40% absolute (Dynes et al. 2006b). The percentage of the protein and lipid in single cells was estimated by converting the integrated thickness of these components for a single cell to a mass (g), which was then divided by the estimated mass (g) of a single cell. To convert integrated thickness to mass involved multiplying the integrated thickness by the area and the density of the biomacromolecules. The density assumed for protein was 1.35 g/cm^3 (Fischer et al. 2004) and the density assumed for lipid was 1.2 g/cm^3 (Okuyama et al. 1984). The single cell dry mass was calculated from the volume of single cells and the wet cell density, assuming that the cell was 70% water (Ingraham et al. 1983). The following formula was used to calculate the volume (V) from the length (l) and width (w) of the bacterial cells: $V = [w^2(\pi/4)(l - w)] + [\pi(w^3/6)]$ (Loferer-Krössbacher et al. 1998). The bacteria were considered as cylinders with hemispherical ends at each side. The formula works equally well for cocci and rods, since $(l - w)$ becomes zero for cocci. The average cell density (wet) was assumed to be 1.1 g/cm^3 (Bjørnsen and Riemann 1988). The protein/lipid ratio was determined from the protein and lipid integrated thickness. All image and spectral processing was performed with aXis2000 (Hitchcock 2007).

The morphological characteristics (length and width) of the bacteria cells for each treatment were also determined from the biology maps. The biology maps are the difference of OD images recorded at 288.2 eV (peak of the C 1s \rightarrow $\pi^*_{\text{C=O}}$ signal of protein) and 282 eV (prior to the onset of the C 1s absorption signal). The length was taken as the long axis and the width as the short axis. Note all stages of bacterial growth were included in the determinations (i.e., including cells at all stages of the cell division cycle). Comparison of the results was conducted with 1-way ANOVA using a commercial statistical software package (MiniTab).

Results

The MIC of the antimicrobial-treated cultures is shown in Table 1. Note that in the TCS-treated *P. fluorescens* culture, growth continued even under saturated TCS conditions (in TSB medium $>30 \mu\text{g/mL}$). Many pseudomonads are intrinsically resistant to TCS; the active ingredient in commercial pseudomonas isolation agar is TCS (trade name Irgasan).

Confocal laser scanning microscopy (CLSM)

Cell viability and biofilm architecture

The 24 and 96 h *P. fluorescens* biofilms grown in the presence and absence of antimicrobial agents were stained simultaneously with SYTO9 and PI. Figure 1 shows typical CLSM images of the 24 h antimicrobial-treated biofilms, and Table 2 presents the cellular density (% surface area occupied by cells). In terms of the total cellular biomass accumulation in the biofilm (SYTO9 + PI-stained cells), the treatments ranked as follows: control (CON) \geq TCS $>$ TSP \geq CHX $>$ BAC. As a secondary indicator of viability, 5- and 6-carboxyfluorescein diacetate (FDA) was injected into the 24 h antimicrobial-treated and control biofilms. All samples were able to cleave the diacetate in FDA, confirming that metabolically active cells were present in all biofilms.

Figure 2 displays typical CLSM images and depth profiles of the 96 h biofilms stained with SYTO9 and PI, and Table 2 reports the cellular density. Similar to the 24 h biofilms (Fig. 1), most of the cells in the 96 h control and TCS- and TSP-treated biofilms were stained only with SYTO9. The biofilm architecture continued to develop in the 96 h control and TCS-treated biofilms, becoming a thick heterogeneous biofilm with microcolonies and channel structures, whereas the biofilm architecture of the 96 h TSP-treated biofilms remained thin and homogeneous like the 24 h TSP-treated biofilm (Fig. 1), with only slight increases in cellular density (Table 2). The 96 h BAC-treated biofilm was different from the 24 h BAC-treated biofilm, being considerably thicker and more heterogeneous (Fig. 2), developing microcolonies and channel structures like the control and the TCS-treated biofilms. Also, in the 96 h BAC-treated biofilm the majority of cells (~70%) were stained with SYTO9, but only ~25% of the cells in the 24 h BAC-treated biofilm were stained with SYTO9. The cells in the 96 h CHX-treated biofilm all appeared stained by PI, and the biofilm remained thin and relatively homogenous as it had at 24 h. In terms of cellular biomass accumulation in the biofilm (SYTO9 + PI stained cells), the 96 h treatments ranked as follows: BAC $>$ CON \geq TCS $>$ TSP \geq CHX.

The 96 h effluent plate counts (i.e., CFU/mL) are shown in Table 2 and their ranking was CON \geq TCS $>$ TSP $>$ BAC $>$ CHX. The number of CFU released from the control

Table 2. The cellular density (%) as determined by in situ SYTO9 and propidium iodide binding analysis of 24 and 96 h *Pseudomonas fluorescens* biofilms, and the plate counts from the effluent collected from the flow cell tube of 96 h *P. fluorescens* biofilms treated with different antimicrobial agents.

Treatment	Type of binding analysis ^a		
	Cellular density stained by SYTO9 (%)	Cellular density stained by propidium iodide (%)	Plate counts (CFU/mL × 10 ⁴ of effluent solution)
Growth period (24 h)			
Control	23.8±6.8a	0.2±0.2a	ND
Triclosan	19.9±6.7a	0.9±0.9a	ND
Trisodium phosphate	9.6±3.9b	0.9±0.4a	ND
Benzalkonium chloride	0.1±0.1c	0.4±0.1a	ND
Chlorhexidine dihydrochloride	0.0±0.0c	9.5±6.0b	ND
Growth period (96 h)			
Control	24.6±10.8a	0.5±0.6a	4000±2000
Triclosan	21.9±10.0ab	0.4±0.8a	3000±2000
Trisodium phosphate	15.0±5.5b	1.4±1.1a	2±0.1
Benzalkonium chloride	24.3±14.6a	10.9±9.5b	0.2±0.04
Chlorhexidine dihydrochloride	0.0±0.0c	5.0±3.8c	0.005±0.001

Note: CFU, colony forming units; ND, not determined.

^aValues followed by the same letter are not significantly different ($p < 0.05$, $n = 4$). Note that statistical comparisons were made between SYTO9 and PI within each growth period, and not between the 24 and 96 h growth periods.

and TCS-treated biofilms were similar, and ~3 orders of magnitude greater than from the TSP-treated biofilm. The CFU in the BAC-treated biofilm were an order of magnitude less compared with the TSP-treated biofilm and 40 times more than the CHX-treated biofilm.

Chemistry of the extracellular polymeric substances (EPS)

Figure 3 shows CLSM images and depth profiles of the 96 h antimicrobial-treated biofilms stained with fluor-conjugated lectins and Table 3 summarizes the analysis of the amount of lectin binding present in each biofilm. In the control biofilm, binding of the *Triticum*-lectin (red) was observed but not *Vicia*-lectin binding (green). *Triticum*-lectin binding for the TCS-treated biofilm was about twice that of the control biofilm, and the TCS biofilm had extensive *Vicia*-lectin binding EPS concentrated in a layer at the biofilm surface–solution interface. The TSP-treated biofilm appeared dominated by the presence of *Vicia*-lectin binding EPS. The thin CHX-treated biofilm EPS stained with both *Triticum*- and *Vicia*-lectin, co-localization was evident on the cells and microcolonies. For the BAC-treated biofilms, *Triticum*-lectin binding was dominant as in the control biofilms, although the distribution pattern was altered with a loss of the diffuse polymer between the microcolonies.

Scanning transmission X-ray microscopy (STXM)

Biomacromolecule mapping

Figure 4a displays an OD image of a 20 μm × 20 μm region of the untreated control biofilm. This image was recorded in transmission at 288.2 eV, an energy where the absorption is dominated by the strong C 1s → π*_{C=O} band of the amide carbonyl of the protein (Stewart-Ornstein et al. 2007). The spectra of CHX, TCS, and BAC are presented in Fig. 4b.

The spatial distribution of the protein, lipid, and polysac-

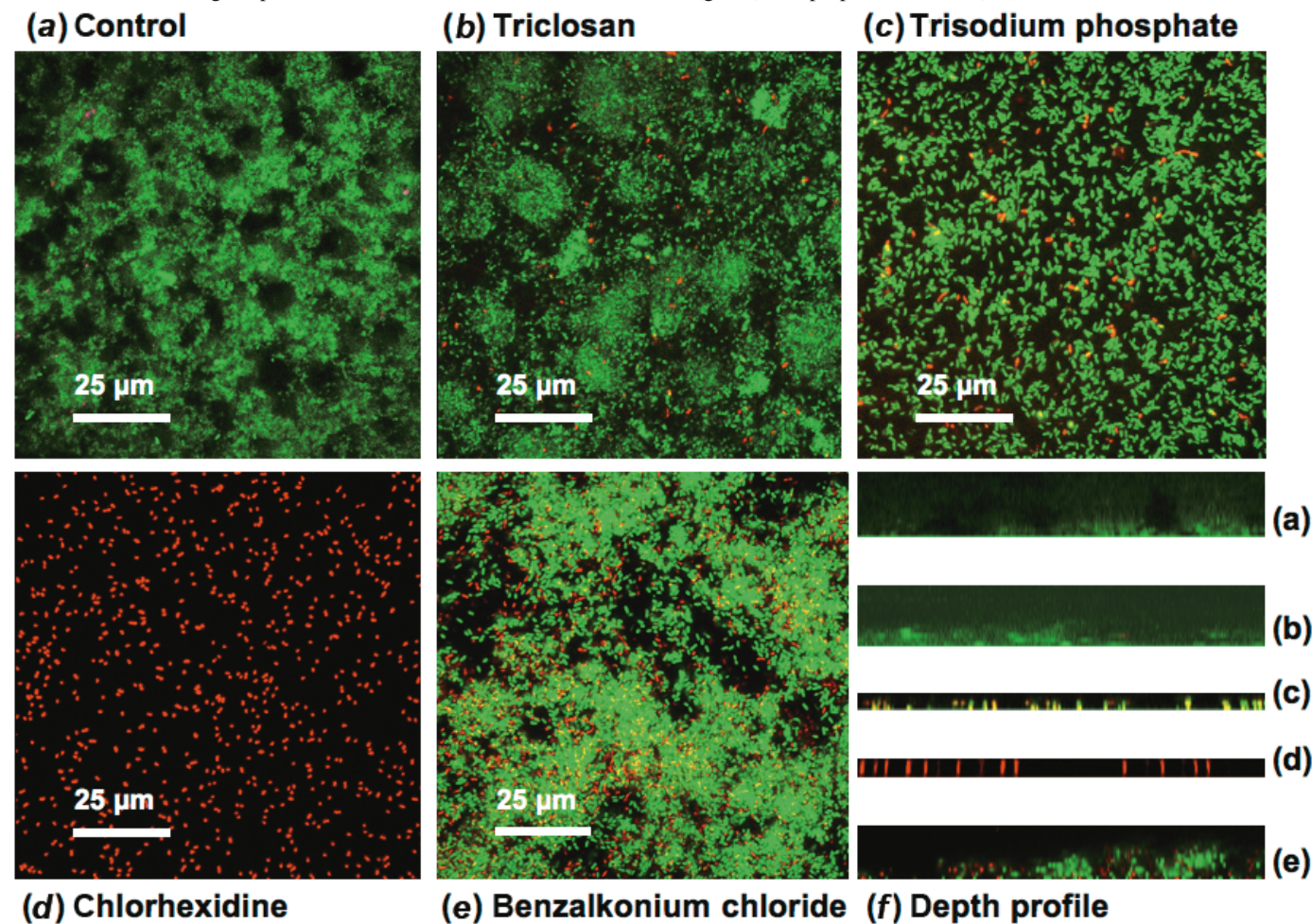
charide in the control and 24 h antimicrobial-treated biofilms are presented as composite color maps (Fig. 5), derived from the component maps (not shown). The relative amounts of protein, lipid, and polysaccharide in the control and 24 h antimicrobial-treated biofilms are listed in Table 4. There were clear differences in the spatial distribution of the protein, lipid, and polysaccharide material between biofilms. The relative amount of protein in the control and antimicrobial-treated biofilms ranged from 25% to 46% in the order TSP > CON ≥ BAC > TCS ≥ CHX. The relative amount of lipid in the biofilms ranged from 20% to 51% in the order BAC > CHX > CON ≥ TCS ≥ TSP. The relative amount of polysaccharide in the biofilms ranged from 15% to 53% in the order TCS > CON ≥ CHX ≥ TSP > BAC.

The percentage of protein and lipids in single bacterial cells in the control and antimicrobial-treated biofilms are listed in Table 5. The percentage of protein in the bacterial cells in these biofilms was similar to that of the control, except for the TCS-treated biofilm, which was higher. The cellular protein percentage followed the order TCS > CON ≥ TSP ≥ BAC ≥ CHX. The percentage of lipids in the cells of antimicrobial-treated and control biofilms varied from 5% to 26% and followed the order TCS > CHX ≥ BAC > TSP ≥ CON. The protein/lipid ratio trend was CON > TSP > BAC ≥ TCS ≥ CHX.

Cell morphology

The length and width (morphology) of the bacterial cells in the 24 h biofilms were determined from the 288.2 eV biology maps (similar to those in Fig. 4a). Quantitative analyses of the cell morphology are summarized in Table 6. The characteristic shape of the cells in the absence of antimicrobial agents (i.e., control) was rod shaped ($l:w = 2.5$). In contrast, the cells in the presence of CHX and TSP were coccoid shaped ($l:w = 1.4-1.5$). Compared with the control, the width of cells from the TCS-treated biofilm was consid-

Fig. 2. Confocal laser scanning microscopy images and depth profiles of 96 h *Pseudomonas fluorescens* biofilms grown in the presence and absence of antimicrobial agents. (a) Control, (b) triclosan (TCS), (c) trisodium phosphate (TSP), (d) chlorhexidine dihydrochloride (CHX), (e) benzalkonium chloride (BAC), and (f) depth profiles of biofilms. The letters (a–e) in (f) correspond to the same antimicrobial agent as indicated in each image caption. The biofilms were stained with SYTO9 (green) and propidium iodide (red).



erably reduced, whereas its length was similar, with a l/w ratio of 3.6. The morphology of the BAC-treated cells was similar to that of the control ($l:w = 2.3$).

Chlorhexidine mapping

The TCS and BAC C 1s spectra were too similar to that of the biomacromolecules spectra (Lawrence et al. 2003; Dynes et al. 2006b) to permit derivation of TCS and BAC component maps. Chlorhexidine was mapped in the 24 h biofilm and was associated with the lipids in the cell (Fig. 6). The STXM detection limit for CHX was estimated by adding its spectrum to that of the major biomacromolecules over a range of compositions. The detection limit was based on the visibility of the characteristic sharp features at 285.1 and 286.4 eV, associated with $C\ 1s \rightarrow \pi^*_{\text{ring}}$ and $C\ 1s \rightarrow \pi^*_{C=N}$ transitions in the phenyl and imide groups of chlorhexidine against the background spectrum of the other species. It was found that these 2 spectral features were readily discernable at a level of 10 nm of CHX combined with the spectrum of 50 nm of protein or 100 nm of lipid, and at a level of 20 nm against a background combination spectrum of 50 nm protein and 100 nm lipid. While the fractional sensitivity is not that exceptional, the absolute sensitivity is im-

pressive, since an average thickness of 10 nm of chlorhexidine in a 500 nm high and 50 nm diameter column (1 pixel) corresponds to $\sim 1 \times 10^{-17}$ mol assuming the density of pure CHX is 1.2 g/cm³.

Figure 7 presents the results of a curve fit to the spectrum of a CHX-rich region (extracted from pixels with a CHX thickness >40 nm) of the CHX-treated biofilm. Comparison with the fit with and without the CHX component clearly indicates the spectral basis of the mapping capability.

Discussion

The inhibitory activity of many antimicrobial agents requires that the integrity of the cell membrane must be compromised through the insertion of the antimicrobial agent in the cell membrane, leading to leakage of cytoplasmic materials or penetration of the compound into the cell, affecting internal processes (McLandsborough et al. 2006). Leakage of low molecular mass cytoplasmic constituents can be an indication of irreversible disorganization of the cytoplasmic membrane (Gilbert et al. 1977; Sampathkumar et al. 2003). We were unable to confirm whether there was leakage of cytoplasmic materials or damaged membranes using STXM,

Fig. 3. Confocal laser scanning microscopy images and depth profiles of 96 h *Pseudomonas fluorescens* biofilm grown in the presence and absence of antimicrobial agents. (a) Control, (b) triclosan (TCS), (c) trisodium phosphate (TSP), (d) chlorhexidine dihydrochloride (CHX), (e) benzalkonium chloride (BAC), and (f) depth profiles of biofilms. The letters (a–e) in (f) correspond to the same antimicrobial agent as indicated in each image caption. The biofilms were stained with the lectins *Triticum vulgare* (red) and *Vicia villosa* (green).

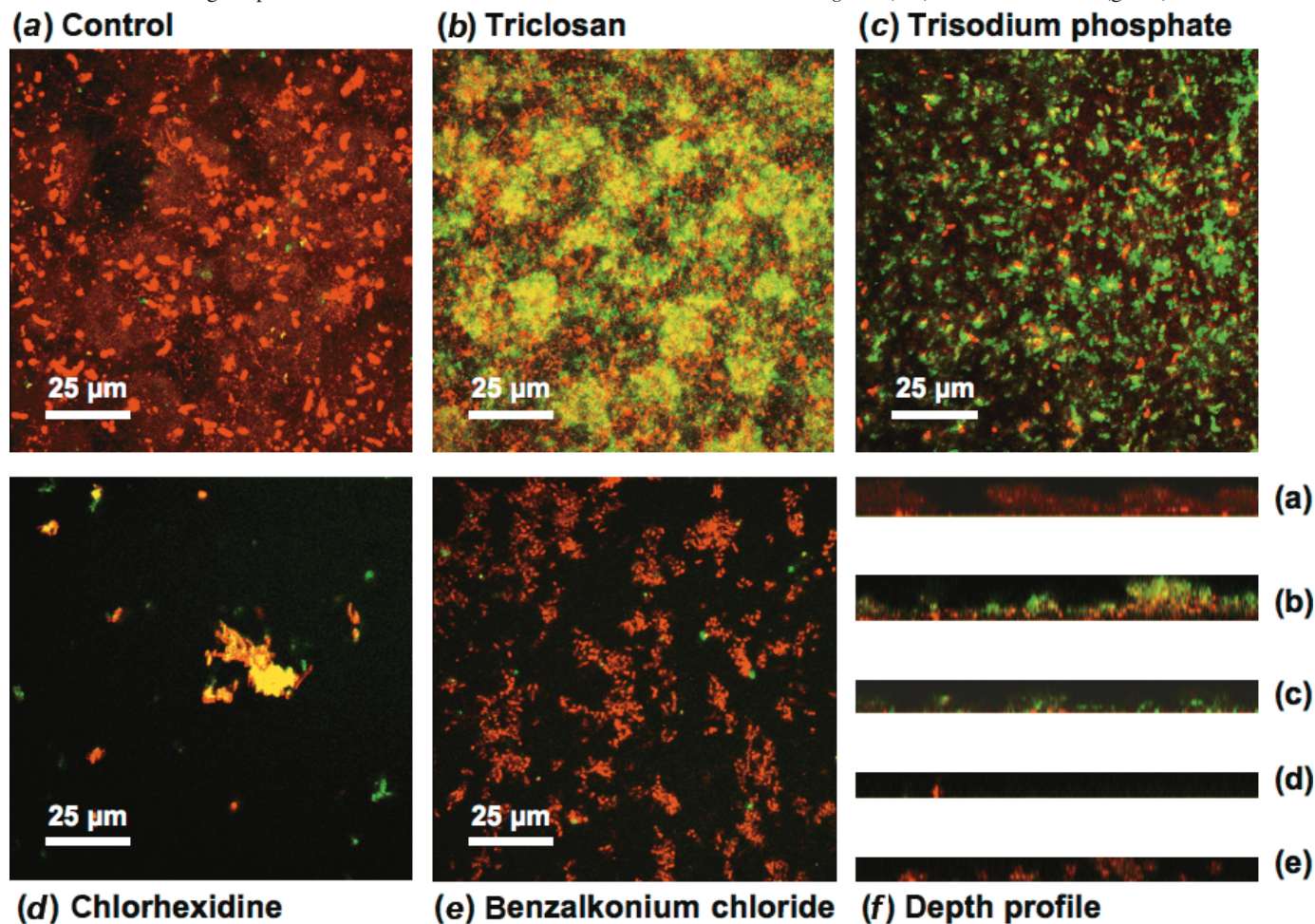


Table 3. The volume per unit area coverage of different biofilm exopolymers as determined by in situ lectin binding analysis of 96 h *Pseudomonas fluorescens* biofilms treated with different antimicrobial agents.

Treatment	Type of lectin binding analysis ^a	
	<i>Triticum vulgare</i> ($\mu\text{m}^3/\mu\text{m}^2$)	<i>Vicia villosa</i> ($\mu\text{m}^3/\mu\text{m}^2$)
Control	1.5b \pm 0.9	0.0a \pm 0.0
Triclosan	3.4c \pm 0.4	2.7c \pm 1.4
Trisodium phosphate	0.3a \pm 0.1	0.7b \pm 0.2
Benzalkonium chloride	0.5a \pm 0.1	0.0a \pm 0.0
Chlorhexidine dihydrochloride	0.1a \pm 0.1	0.1a \pm 0.1

^aValues followed by the same letter are not significantly different ($p < 0.05$, $n = 4$).

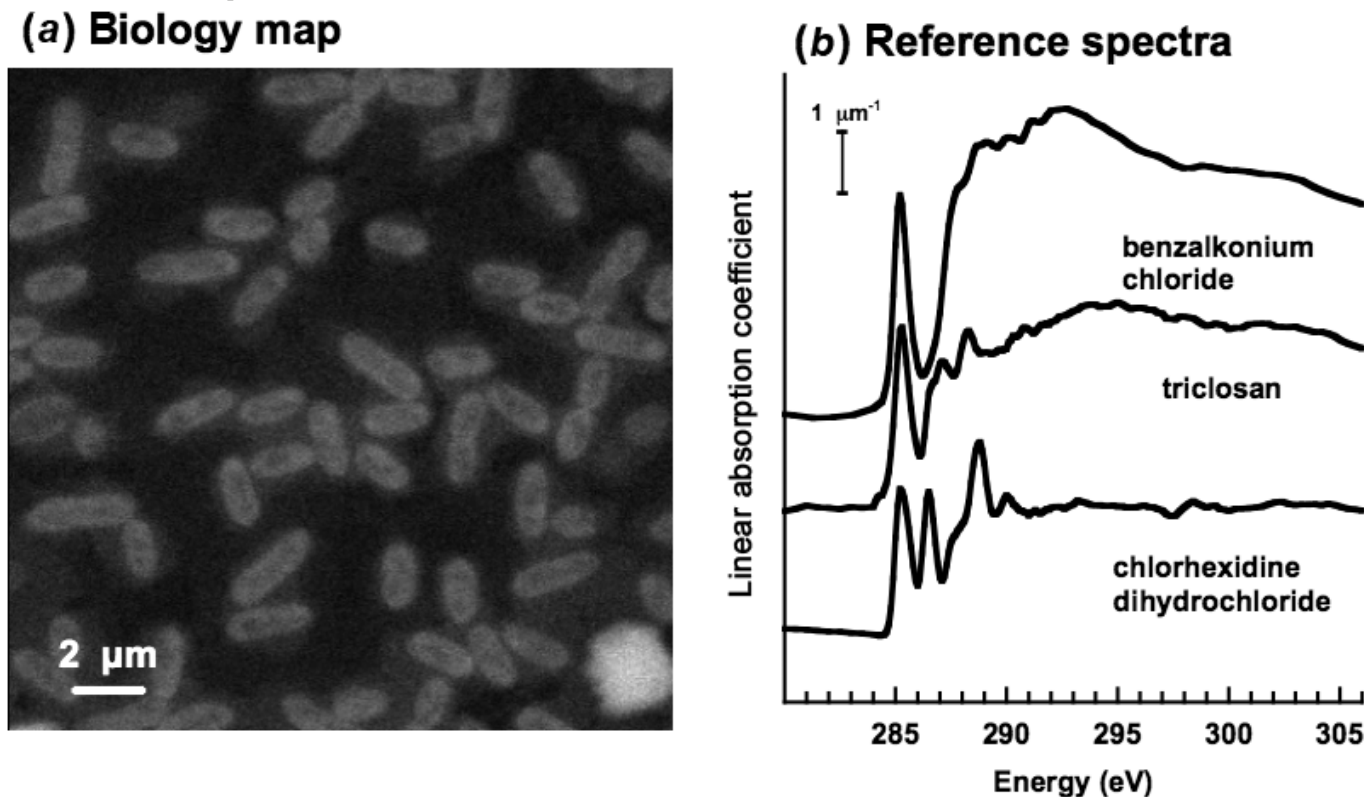
as their expected concentrations and membrane alterations were below the detection limit ($\sim 1 \times 10^{-17}$ mol) and the spatial resolution (~ 25 nm) of STXM.

Growth inhibition by antimicrobials does not always depend upon the loss of intracellular constituents, but instead results from, at least in part, membrane structural perturba-

tions that, while not always drastic enough to perforate the membrane, nonetheless interfere with normal membrane functions (Guillén et al. 2004). Correlation of the cellular membrane integrity with the cellular density and biofilm architecture can give insights into possible modes of antimicrobial action. The membrane of the cells in the 24 and 96 h TCS-treated biofilms were unaffected, indicating that the TCS had not affected the cell membrane. Cell membrane integrity was compromised in all cells in the 24 and 96 h CHX-treated biofilm (Figs. 1 and 2). The CHX-treated biofilm also had the lowest cellular density and poorly developed biofilm structure (Table 2). Chlorhexidine has been shown to alter the outer membrane and cytoplasm of *Candida albicans* (Ellepolá and Samaranayake 1998). Our results are consistent with membrane damage, confirming that *P. fluorescens* is sensitive to CHX. Nevertheless, the FDA analysis of 24 h biofilms indicated the presence of metabolically active cells, and the effluent plate counts from the 96 h biofilms (Table 2) further confirmed the presence of viable cells.

The low percentage ($\sim 10\%$) of PI-stained cells in the 24 and 96 h TSP-treated biofilms (Figs. 1 and 2) indicated that the cell membrane of most cells was not compromised.

Fig. 4. (a) Biology map (288.2–280 eV OD images) of the control biofilm of a 20 $\mu\text{m} \times 20 \mu\text{m}$ area. (b) C 1s X-ray absorption (NEXAFS) reference spectra of the antimicrobial agents. The spectra of triclosan (TCS), benzalkonium chloride (BAC), and chlorhexidine dihydrochloride (CHX) are plotted on an absolute linear absorbance scale with offset.



However, the thin biofilm and lower cellular density compared with the control indicated a reduced viability and reproduction of the biofilm cells. Sampathkumar et al. (2003), using TEM, showed that the treatment of planktonic *Salmonella enterica* serovar Enteritidis cells with 1.5%–2.5% TSP (compared with 0.1% TSP, pH 11 used in this study) resulted in the disruption and perforation of the outer and cytoplasmic membranes largely because of the alkaline pH (~11), which in turn leads to loss of intracellular contents. Thus, it appears that most cells in the TSP-treated biofilm were resistant to the alkaline pH, although the cells were stressed. In the BAC-treated biofilms the percentage of membrane-compromised cells changed with time from ~70% of the cells at 24 h to ~25% of the cells at 96 h. However, while the cellular density of the 24 h BAC-treated biofilm was considerably less than the 24 h control biofilm, it was similar to that of the control and TCS-treated biofilm at 96 h (Fig. 2). Other researchers (Langsrud et al. 2003; Braoudaki and Hilton 2005; Mangalappalli-Illathu and Korber 2006; Bore et al. 2007) have shown that repeated exposures of various bacterial genera to increasing sub-MIC of BAC resulted in adaptation or the acquisition of resistance. Our observations suggest that some BAC-treated cells had undergone adaptation over time in situ.

There is continuous interaction and exchange between biofilm and planktonic populations (attachment, detachment, and reattachment), and studies sampling planktonic populations have shown they were representative of the biofilm population (Holm et al. 1992; Wolfaardt et al. 1994b).

Thus, the number of viable cells released in the effluent (determined by plating on agar) provides an index of biofilm cell viability. Our viability results were in good agreement with the 96 h cellular biomass accumulation (i.e., cellular density; Table 2), except for the BAC-treated biofilm in which an increase in biomass did not result in an increase of viable cells in the effluent. The change in BAC biofilms between 24 and 96 h in terms of viability and biomass may be the consequence of BAC adaptation of *P. fluorescens* biofilm cells.

Bacteria respond to environmental stress by altering their cellular morphology, a phenomenon believed to permit continued cell growth and division (Young 2003, 2006). For example, Cefali et al. (2002) studied the response of *Pseudomonas aeruginosa* during nutrient starvation and they observed that the normally rod-shaped cells became smaller and coccoid shaped. It was suggested that the shape change was linked to the stationary phase and reduced energy requirements to cope with unfavorable conditions. Other researchers (Givskov et al. 1994; van Overbeek et al. 1995; Rowan 1999; Jan et al. 2001; Steinberger et al. 2002) have shown that the characteristic cell morphology of stressed bacteria (starvation and pH) is also altered. Watkin et al. (2003) showed that a decrease in pH from 7 to 4.8 resulted in *Rhizobium leguminosarum* cells becoming shorter and wider, while maintaining a similar l/w ratio, relative to an acid-sensitive mutant strain that did not change cell morphology. In the presence of CHX and TSP, the *P. fluorescens* used in this study also changed from the normal rod

Fig. 5. Color composite maps (rescaled) of the protein (red), polysaccharide (green), and lipid (blue) spatial distribution in *Pseudomonas fluorescens* biofilms grown in the presence and absence of antimicrobial agents, derived from the composite maps (not shown). (a) Control, (b) triclosan (TCS), (c) trisodium phosphate (TSP), (d) chlorhexidine dihydrochloride (CHX), and (e) benzalkonium chloride (BAC).

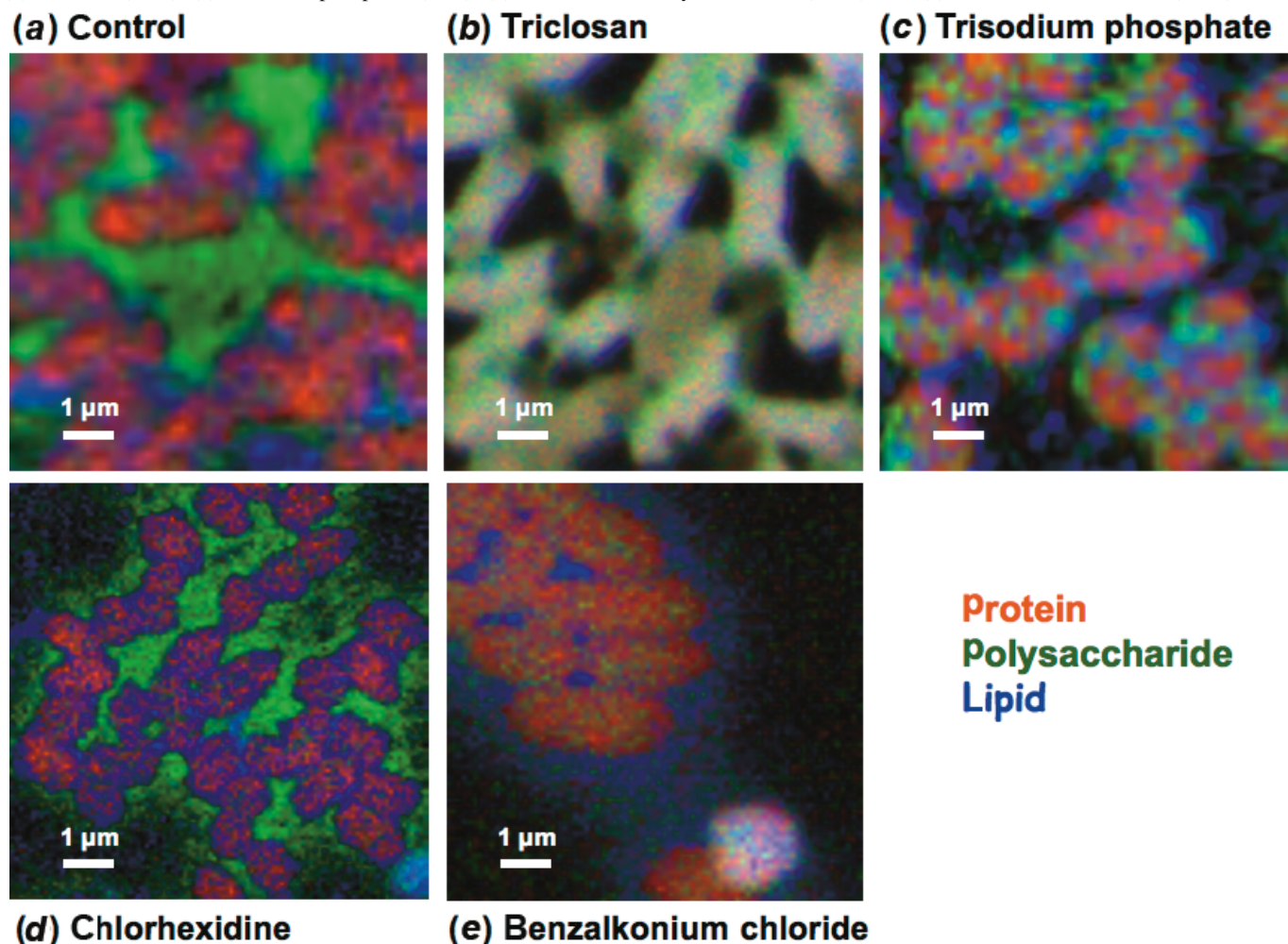


Table 4. Relative amounts of the biomacromolecules in *Pseudomonas fluorescens* biofilms in the 24 h biofilms treated with different antimicrobial agents.

Treatment	Relative amount in the biofilm (%) ^a		
	Protein	Lipid	Polysaccharide
Control	36	24	40
Benzalkonium chloride	34	51	15
Triclosan	25	22	53
Trisodium phosphate	46	20	34
Chlorhexidine dihydrochloride	25	36	40

^aPercentages may not total 100% owing to rounding. The maximum error associated with each determination is estimated to be about 10% relative and 40% absolute. The antimicrobial agent signals were not accounted for in the relative amounts.

shape to a coccoid shape (Table 6), which is consistent with a stress response. Interestingly, despite the fact that the *P. fluorescens* was resistant to TCS, the cell shape changed, although in the BAC biofilms the cells were not significantly different from the control in keeping with the suggestion that adaptation to BAC had occurred.

In this study STXM allowed the determination of the total concentration and distribution of the proteins and lipids in the individual cells (Table 5 and Fig. 5). The concentration of protein in single cells is expected to be 40%–60% of the total dry mass (*m/m* basis) (Ingraham et al. 1983). The percent protein determined by our method appears to be less than this, in some cases by as much as a factor of 2–3. The expected amount of lipid in bacterial cells varies from 10% to 35% (Anderes et al. 1971; Ingraham et al. 1983), thus, our results are in keeping with previous studies.

There is some indication that the spatial arrangement of protein assemblies influences biochemical processes (e.g., correctly localizing synthetic enzymes) within the cell, such as those involving bacterial morphology (Young 2003, 2006). There was also a change in the spatial distribution of protein and lipid in the cells in the antimicrobial-treated biofilms. However, the detailed relationship between the spatial distribution of protein and lipid and response to antimicrobial agents remains to be determined.

Following exposure to antimicrobial agents, there is often a modification of the biomacromolecular composition and quantity in the biofilm and bacterial cells. For example, López-Diez et al. (2005) monitored the effects of amikacin on

Table 5. Amounts and percentages of protein and lipid, the protein/lipid ratios, and the cell volumes and masses for *Pseudomonas fluorescens* single bacterial cells in the 24 h biofilms treated with different antimicrobial agents.

Treatment	Cell volume (μm^3) ^{a,b}	Cell dry mass ($\text{g} \times 10^{-13}$) ^{b,c}	Total cellular protein mass ($\text{g} \times 10^{-14}$) ^{b,d}	Percentage of protein ^{b,e}	Total cellular lipid mass ($\text{g} \times 10^{-14}$) ^b	Percentage of lipid ^b	Protein/lipid ratio ^b
Control	1.1±0.2b	3.8±0.7b	6.8±1.5c	18±3a	1.9±0.1a	5±2a	3.9±0.2d
Benzalkonium chloride	1.0±0.3b	3.5±1.4b	5.0±1.8b	15±2a	3.2±0.3b	10±3b	1.5±0.2b
Triclosan	0.6±0.2a	2.0±0.7a	7.3±1.5c	29±9b	4.6±1.3c	26±12c	1.2±0.2ab
Trisodium phosphate	0.7±0.4a	2.4±1.2a	3.3±0.8ab	16±5a	1.2±0.1a	6±2a	2.7±0.3c
Chlorhexidine dihydrochloride	0.7±0.1a	2.2±0.1a	3.2±0.6ab	15±1a	3.2±0.3b	15±2b	1.0±0.3a

^aValues followed by the same letter are not significantly different ($p < 0.05$, $n = 4$).

^bVolume (V) calculated from the length (l) and width (w) of the bacterial cells: $V = [(w^2\pi/4)(l - w)] + [\pi(w^3/6)]$ (Loferer-Krössbacher et al. 1998). The bacteria were considered as cylinders with hemispherical ends at each side.

^cAssumes the average wet cell density was 1.1 g/cm^3 (Bjørnsen and Riemann 1988) and that the cell was 70% water (Ingraham et al. 1983).

^dAssumes the density of protein was 1.35 g/cm^3 (Fischer et al. 2004) and the density for lipids was 1.2 g/cm^3 (Okuyama et al. 1984).

^eTotal cellular biomacromolecule mass/cell dry mass.

Table 6. Morphological characteristics of the *Pseudomonas fluorescens* cells from 24 h biofilms treated with different antimicrobial agents.

Treatment	Mean length (μm) ^{a,b}	Mean width (μm) ^{a,b}	Length:width ratio
Control	2.2±0.5b	0.9±0.1b	2.5
Benzalkonium chloride	2.1±0.4b	0.9±0.1b	2.3
Triclosan	2.1±0.4b	0.6±0.1a	3.6
Trisodium phosphate	1.5±0.3a	1.0±0.1c	1.5
Chlorhexidine dihydrochloride	1.4±0.3a	1.0±0.1c	1.4

Note: Determined from the 288.2 eV biology maps.

^aLength is defined as the long axis and width is defined as the short axis.

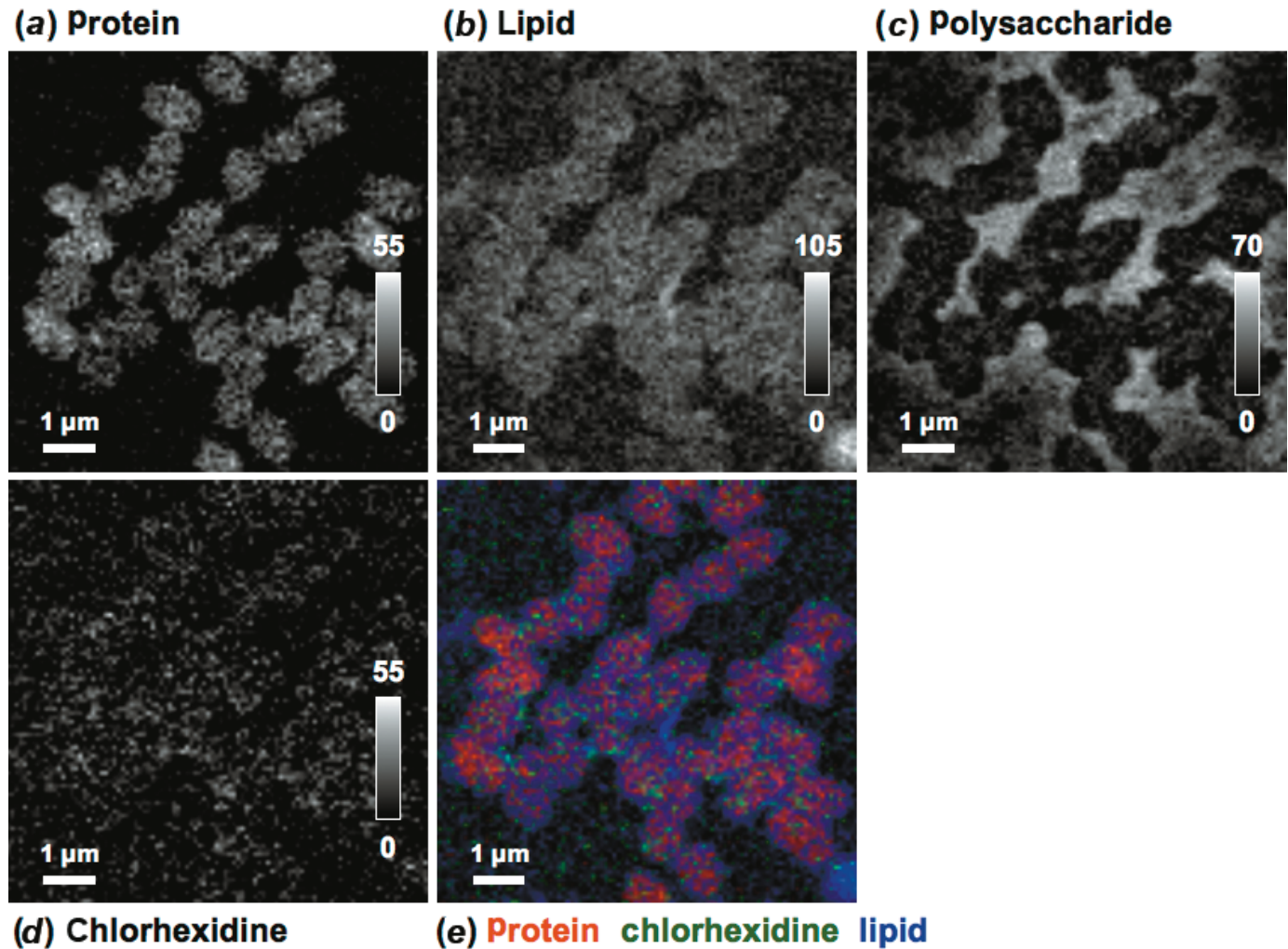
^bValues followed by the same letter are not significantly different ($p < 0.05$, $n = 40$).

P. aeruginosa under sub-MIC conditions using Raman spectroscopy. They found that as the concentration of amikacin was increased, the protein-related peaks decreased while the nucleic acid-related peaks increased. A study of a *P. aeruginosa* biofilm exposed to quaternary ammonium compounds (QAC) (BAC belongs to this group) showed modifications of the fatty acid composition indicating that the antimicrobial agent was interacting with the cell membrane (Guérin-Méchin et al. 1999; Méchin et al. 1999). Moreover, resistant cells of *P. aeruginosa* averaged 77% more total lipid versus sensitive cells when grown in the presence of QAC, and even in the absence of the QAC averaged 27% more lipid than the sensitive cells (Anderes et al. 1971). Tattawasart et al. (2000a, 2000b) reported that a CHX-resistant *Pseudomonas stutzeri* exhibited up- and down-regulation of protein and lipopolysaccharide material. In our study the increase in lipid content in the cells from the TCS-, CHX-, and BAC-treated biofilms could reflect the overall importance of lipid in bacterial cells and their role in the maintenance of the cell envelope. McMurry et al. (1998) demonstrated that TCS blocks lipid synthesis, thus, the high lipid content in the TCS-treated biofilm is consistent with resistance to TCS. Mooney (2006) studied the same *P. fluorescens* strain used in this study and showed that in the presence of TCS 47 new proteins were produced, 67 of the common proteins were upregulated, and 23 were downregulated. The increase

in protein content of the cells in the TCS-treated biofilm is in keeping with the protein changes observed by Mooney.

Biofilm EPS may act as a diffusion barrier, molecular sieve, and an adsorbent (Suci et al. 1994; Laspidou and Rittman 2002; Prakash et al. 2003), thereby providing a physical-chemical barrier to antimicrobials and preventing their penetration to the cell envelope. Environmental conditions (nutrients, pH, temperature, growth medium and substratum, and age) are known to influence the composition and quantity of exopolymeric substances produced by bacterial biofilms (Wolfaardt et al. 1999). Therefore, alterations in EPS glycoconjugate composition may represent an adaptive response to antimicrobial agents. For example, *Staphylococcus* spp. biofilms grown in the presence of the sub-MIC of dicloxacillin showed a change in spatial structure and composition of the biofilm matrix when examined by CLSM (Cerca et al. 2005). In this study we utilized fluorescent lectin binding analyses and STXM to assess changes in the glycoconjugate quantity and composition of antimicrobial-treated biofilms. *Pseudomonas fluorescens* produced different EPS compositions in response to the antimicrobials (Figs. 3–5; Tables 3 and 4). STXM showed that the highest quantity of EPS was in the 24 h TCS-treated biofilm. CLSM showed that at 96 h TCS-treated biofilms had extensive EPS and different layers with differing compositions (Fig. 3). It was apparent that there were 2 types of EPS occurring as

Fig. 6. Component maps for (a) protein; (b) lipid; (c) polysaccharides; (d) chlorhexidine (CHX), derived by singular value decomposition, for the chlorhexidine-treated biofilm; and (e) color composite map (rescaled; red, protein; green, chlorhexidine; and blue, lipid) of selected component maps. The gray scale (a–d) indicates quantitative thickness (nm).



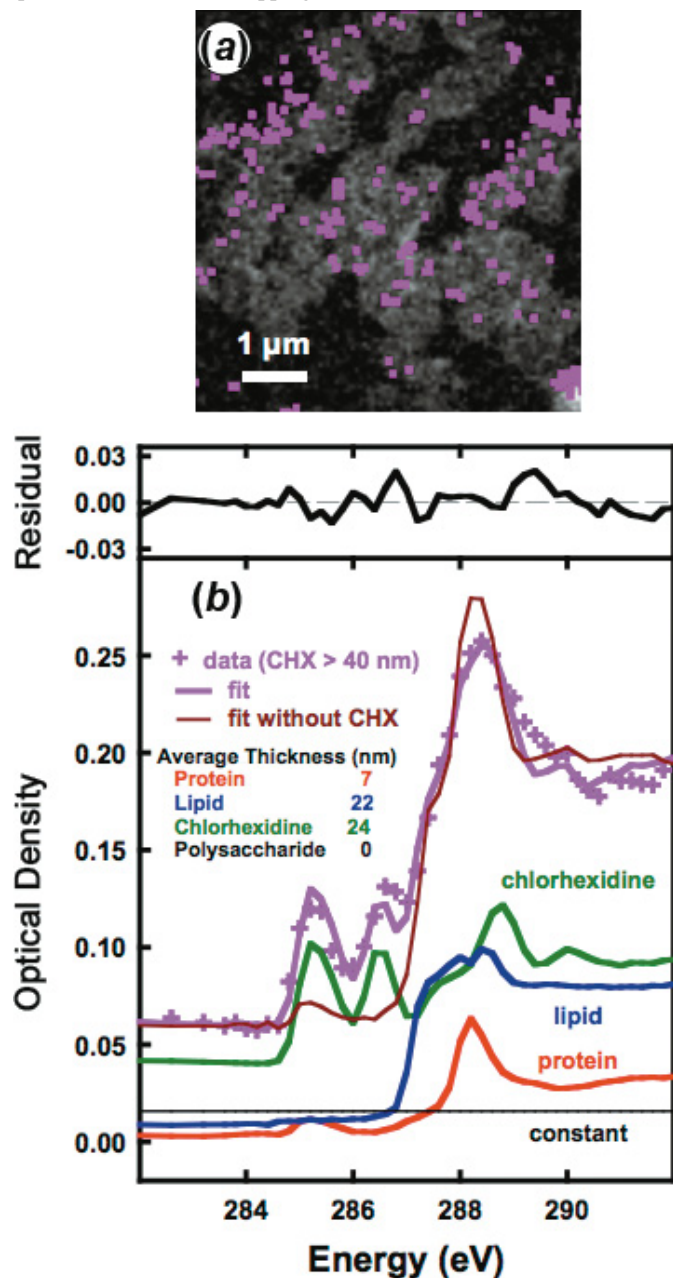
distinct layers in the 96 h TCS-treated biofilm versus only 1 EPS type in the control. This suggests that the TCS-treated biofilm produced an EPS that contributed to the protection from the TCS. The fact that the cell membrane remained undamaged is in keeping with the contention that a protective environment may be created by EPS. The capacity to alter EPS composition may be part of intrinsic resistance to antimicrobials for pseudomonads and other bacteria.

Relative to the TCS-treated biofilm, the CHX-treated biofilm had a very thin layer of EPS with a limited matrix surrounding the cells, as indicated by lectin staining (Fig. 3d). In contrast, STXM indicated that there was EPS between the cells (Fig. 5d) and it comprised ~40% of the biomacromolecules detected. The extensive membrane damage revealed by the PI staining indicated that the cells had been compromised, suggesting that the EPS did not provide protection from CHX. The low cell densities further suggest that CHX may also interfere with the cell adhesion processes, and thus biofilm formation and maintenance. Similarly, sub-MIC of dicloxacillin interfered in cell attachment, causing a reduction in cell density and the production of thin biofilms relative to the control (Cerca et al. 2005). Viable cells were

detected in the TSP-treated biofilm; whereas lectin staining indicated a change in the EPS composition versus the control. These observations parallel TCS, again suggesting an important role for EPS in *P. fluorescens* resistance to antimicrobials. Although EPS has often been postulated as having an important role in bacterial resistance to antimicrobials, it is increasingly clear that modifications to the EPS composition and quantity are an important component of resistance. In the BAC-treated biofilm, EPS production increased with time, as was evident from the STXM 24 h studies and lectin staining of 96 h biofilms. Unlike the TCS-treated biofilm, only 1 EPS type was detected and it was stained by *T. vulgaris* as in the control. Mangalappallilathu et al. (2008) observed changes in composition and quantity of EPS in *Salmonella enterica* serovar Enteritidis biofilms exposed to BAC. These results are again in keeping with adaptation of the bacteria to BAC during this exposure period, albeit without detection of change in EPS composition as observed for TCS.

STXM detected CHX in the biofilm and showed that it was spatially localized, mainly in association with the cell lipid material (Fig. 5). Previously, CHX was found to be as-

Fig. 7. (a) Chlorhexidine (CHX) component map, with pixels having values >40 nm in pink, superimposed on the lipid component map. (b) Curve fit to the spectrum extracted from these pixels. The average thickness (nm) of the major components is indicated. Comparison of the fit quality with and without the CHX component clearly shows the improvement in the fit and thus the basis for the quantitative chemical mapping.



sociated with lipid storage vesicles in 2 diatom species and a bacterial microcolony from a river biofilm (Dynes et al. 2006b). The authors suggested that the binding of CHX to lipids in this manner may interfere with its antimicrobial activity, providing a degree of protection for the cell.

In summary, exposure of *P. fluorescens* biofilms to the sub-MICs of 4 antimicrobial agents resulted in the modification of overall biofilm architecture, EPS composition, cell viability, cell morphology, and redistribution of cellular bio-

macromolecules. STXM allowed high-resolution imaging, with detailed mapping of the biofilm and cell structure and composition, in conjunction with the localization of specific biomacromolecules and the antimicrobial agent CHX. However, STXM did not allow identification and localization of other antimicrobial agents. Additional effort will be required to link the patterns of macromolecular distribution to antimicrobial response and effects. This approach allowed a quantitative analysis of the multifaceted response of *P. fluorescens* to antimicrobial exposure and points to the need for broader evaluation of the role of EPS in both adaptation and resistance.

Acknowledgements

This work was supported by the Advanced Food and Materials Network (AFMNet), Environment Canada, Natural Sciences and Engineering Research Council of Canada (NSERC), and the Canada Research Chair program (APH). Construction and operation of the STXM5.3.2 microscope was supported by National Science Foundation grant NSF DMR-9975694, Department of Energy grant DOE DE-FG02-98ER45737, Dow Chemical, NSERC, and the Canadian Foundation for Innovation. We thank T. Tyliczszak and D. Kilcoyne for their contributions to developing and maintaining the instrument. The Advanced Light Source is supported by the Director, Office of Energy Research, Office of Basic Energy Sciences, Materials Sciences Division of the United States Department of Energy, under contract No. DE-AC03-76SF00098.

References

- Anderes, E.A., Sandine, W.E., and Elliker, P.R. 1971. Lipids of antibiotic-sensitive and -resistant strains of *Pseudomonas aeruginosa*. *Can. J. Microbiol.* **17**: 1357–1365. doi:10.1139/m71-217. PMID:5003246.
- Bjørnsen, P.K., and Riemann, B. 1988. Towards a quantitative stage in the study of microbial processes in pelagic carbon flows. *Arch. Hydrobiol.* **31**(Suppl.): 185–193.
- Bore, E., Hébraud, M., Chafsey, I., Chambon, C., Skjæret, C., Moen, B., et al. 2007. Adapted tolerance to benzalkonium chloride in *Escherichia coli* K-12 studied by transcriptome and proteome analyses. *Microbiology*, **153**: 935–946. doi:10.1099/mic.0.29288-0. PMID:17379704.
- Braoudaki, M., and Hilton, A.C. 2005. Mechanism of resistance in *Salmonella enterica* adapted to erythromycin, benzalkonium chloride, and triclosan. *Int. J. Antimicrob. Agents*, **25**: 31–37. doi:10.1016/j.ijantimicag.2004.07.016. PMID:15620823.
- Breeuwer, P., Drocourt, J., Rombouts, F.M., and Abee, T. 1996. A novel method for continuous determination of the intracellular pH in bacteria with the internally conjugated fluorescent probe 5 (and 6)-carboxyfluorescein succinimidyl ester. *Appl. Environ. Microbiol.* **62**: 178–183. PMID:16535209.
- Caldwell, D.E., and Lawrence, J.R. 1986. Growth kinetics of *Pseudomonas fluorescens* microcolonies within the hydrodynamic boundary layers of surface microenvironments. *Microb. Ecol.* **12**: 299–312. doi:10.1007/BF02011173.
- Cefali, E., Patane, S., Arena, A., Saitta, G., Guglielmino, S., Cappello, S., et al. 2002. Morphological variations in bacteria under stress conditions: near-field optical studies. *Scanning*, **24**: 274–283. PMID:12507381.
- Cerca, N., Martins, S., Sillankorva, S., Jefferson, K.K., Pier, G.B., Oliveira, R., and Azeredo, J. 2005. Effects of growth in the pre-

- sence of subinhibitory concentrations of dicloxacillin on *Staphylococcus epidermidis* and *Staphylococcus haemolyticus* biofilms. *Appl. Environ. Microbiol.* **71**: 8677–8682. doi:10.1128/AEM.71.12.8677-8682.2005. PMID:16332862.
- Cheung, H.-Y., Chan, G.K.-L., Cheung, S.-J., Sun, S.-Q., and Fong, W.-F. 2007. Morphological and chemical changes in the attached cells of *Pseudomonas aeruginosa* as primary biofilms develop on aluminium and CaF₂ plates. *J. Appl. Microbiol.* **102**: 701–710. doi:10.1111/j.1365-2672.2006.03137.x. PMID:17309619.
- Dynes, J.J., Lawrence, J.R., Korber, D.R., Swerhone, G.D.W., Leppard, G.G., and Hitchcock, A.P. 2006a. Quantitative mapping of chlorhexidine in natural river biofilms. *Sci. Total Environ.* **369**: 369–383. doi:10.1016/j.scitotenv.2006.04.033. PMID:16777190.
- Dynes, J.J., Tylliszczak, T., Araki, T., Lawrence, J.R., Swerhone, G.D.W., Leppard, G.G., et al. 2006b. Quantitative mapping of metal species in bacterial biofilms using scanning transmission X-ray microscopy. *Environ. Sci. Technol.* **40**: 1556–1565. doi:10.1021/es0513638. PMID:16568770.
- Ellepol, A.N., and Samaranyake, L.P. 1998. The effect of limited exposure to antimycotics on the relative cell-surface hydrophobicity and the adhesion of oral *Candida albicans* to buccal epithelial cells. *Arch. Oral Biol.* **43**: 879–887. doi:10.1016/S0003-9969(98)00064-8. PMID:9821511.
- Fischer, H., Polikarpov, I., and Craievich, A.F. 2004. Average protein density is a molecular-weight-dependent function. *Protein Sci.* **13**: 2825–2828. doi:10.1110/ps.04688204. PMID:15388866.
- Gilbert, P., Beveridge, E.G., and Crone, P.B. 1977. The lethal action of 2-phenoxyethanol and its analogues upon *Escherichia coli* NCTC 5933. *Microbiology*, **19**: 125–141.
- Givskov, M., Eberl, L., Moller, S., Poulsen, L.K., and Molin, S. 1994. Responses to nutrient starvation in *Pseudomonas putida* KT2442: analysis of general cross-protection, cell shape, and macromolecular content. *J. Bacteriol.* **176**: 7–14. PMID:8282712.
- Guérin-Méchin, L., Dubois-Brissonnet, F., Heyd, B., and Leveau, J.Y. 1999. Specific variations of fatty acid composition of *Pseudomonas aeruginosa* ATCC induced by quaternary ammonium compounds and relation with resistance to bactericidal activity. *J. Appl. Microbiol.* **87**: 735–742. doi:10.1046/j.1365-2672.1999.00919.x. PMID:10594715.
- Guillén, J., Bernabeu, A., Shapiro, S., and Villalain, J. 2004. Location and orientation of triclosan in phospholipids model membranes. *Eur. Biophys. J.* **33**: 448–453. doi:10.1007/s00249-003-0378-8. PMID:14714154.
- Hadjok, C., Mittal, G.S., and Warriner, K. 2008. Inactivation of human pathogens and spoilage bacteria on the surface and internalized within fresh produce by using a combination of ultraviolet light and hydrogen peroxide. *J. Appl. Microbiol.* **104**: 1014–1024. doi:10.1111/j.1365-2672.2007.03624.x. PMID:18248373.
- Henke, B.L., Gullikson, E.M., and Davis, J.C. 1993. X-ray interactions: photoabsorption, scattering, transmission, and reflection at $E = 50\text{--}30,000$ eV, $Z = 1\text{--}92$. *At. Data Nucl. Data Tables*, **54**: 181–342. doi:10.1006/adnd.1993.1013.
- Hitchcock, A.P. 2007. Analysis of X-ray images and spectra (aXis2000) [computer program]. Available from <http://unicom.mcmaster.ca/aXis2000.html>.
- Hitchcock, A.P., Morin, C., Heng, Y.M., Cornelius, R.M., and Brash, J.L. 2002. Towards practical soft X-ray spectromicroscopy of biomaterials. *J. Biomater. Sci. Polym. Ed.* **13**: 919–938. doi:10.1163/156856202320401960. PMID:12463511.
- Holm, P.E., Nielsen, P.H., Albrechtsen, H.-J., and Christensen, T.H. 1992. Importance of unattached bacteria and bacteria attached to sediment in determining potentials for degradation of xenobiotic organic contaminants in an aerobic aquifer. *Appl. Environ. Microbiol.* **58**: 3020–3026. PMID:1444415.
- Ingraham, J.L., Maaloe, O., and Neidhardt, F.C. 1983. Composition, organization, and structure of the bacterial cell. *In* Growth of the bacterial cell. Sinauer Associates Inc., Sunderland, Mass. Chap. 1. pp. 1–48.
- Jacobsen, C., Wirrick, S., Flynn, G., and Zimba, C. 2000. Soft X-ray spectroscopy from image sequences with sub-100 nm spatial resolution. *J. Microsc.* **197**: 173–184. doi:10.1046/j.1365-2818.2000.00640.x. PMID:11543408.
- Jan, G., Leverrier, P., Pichereau, V., and Boyaval, P. 2001. Changes in protein synthesis and morphology during acid adaptation of *Propionibacterium freudenreichii*. *Appl. Environ. Microbiol.* **67**: 2029–2036. doi:10.1128/AEM.67.5.2029-2036.2001. PMID:11319077.
- Kilcoyne, A.L.D., Steele, W.F., Fakra, S., Hitchcock, P., Franck, K., Anderson, E., et al. 2003. Interferometrically controlled scanning transmission microscopes at the Advanced Light Source. *J. Synchrotron Radiat.* **10**: 125–136. doi:10.1107/S0909049502017739. PMID:12606790.
- Kirsop, B.E., and Snell, J.S.S. 1984. Maintenance of microorganisms: a manual of laboratory methods. pp. 35–40. London: Academic Press.
- Koprinarov, I.N., Hitchcock, A.P., McCrory, C.T., and Childs, R.F. 2002. Quantitative mapping of structured polymeric systems using singular value decomposition analysis of soft X-ray images. *J. Phys. Chem. B*, **106**: 5358–5364. doi:10.1021/jp0132811.
- Korber, D.R., Lawrence, J.R., Sutton, B., and Caldwell, D.E. 1989. Effect of laminar flow velocity on the kinetics of surface recolonization by Mot⁺ and Mot⁻ *Pseudomonas fluorescens*. *Microb. Ecol.* **18**: 1–19. doi:10.1007/BF02011692.
- Korber, D.R., James, G.A., and Costerton, J.W. 1994. Evaluation of fleroxacin activity against established *Pseudomonas fluorescens* biofilms. *Appl. Environ. Microbiol.* **60**: 1663–1669. PMID:16349262.
- Langsrud, S., Sundheim, G., and Borgmann-Strahsen, R. 2003. Intrinsic and acquired resistance to quaternary ammonium compounds in food-related *Pseudomonas* spp. *J. Appl. Microbiol.* **95**: 874–882. doi:10.1046/j.1365-2672.2003.02064.x. PMID:12969304.
- Laspidou, C.S., and Rittman, B.E. 2002. A unified theory for extracellular polymeric substances, soluble microbial products, and active and inert biomass. *Water Res.* **36**: 2711–2720. doi:10.1016/S0043-1354(01)00413-4. PMID:12146858.
- Lawrence, J.R., Korber, D.R., Hoyle, B.D., Costerton, J.W., and Caldwell, D.E. 1991. Optical sectioning of microbial biofilms. *J. Bacteriol.* **173**: 6558–6567. PMID:1917879.
- Lawrence, J.R., Swerhone, G.D.W., Leppard, G.G., Araki, T., Zhang, X., West, M.M., and Hitchcock, A.P. 2003. Scanning transmission X-ray, laser scanning, and transmission electron microscopy mapping of the exopolymeric matrix of microbial biofilms. *Appl. Environ. Microbiol.* **69**: 5543–5554. doi:10.1128/AEM.69.9.5543-5554.2003. PMID:12957944.
- Lawrence, J.R., Korber, D.R., and Neu, T.R. 2007a. Analytical imaging techniques. *In* Manual of environmental microbiology. 3rd ed. Edited by C.J. Hurst, R.L. Crawford, J.L. Garland, D.A. Lipson, A.L. Mills, and L.D. Stetzenbach. American Society for Microbiology Press, Washington, D.C. pp. 40–68.
- Lawrence, J.R., Swerhone, G.D.W., Topp, E., Korber, D.R., Neu, T.R., and Wassenaar, L.I. 2007b. Structural and functional responses of river biofilm communities to the nonsteroidal anti-inflammatory diclofenac. *Environ. Toxicol. Chem.* **26**: 573–582. doi:10.1897/06-340R.1. PMID:17447540.

- Lindsay, D., and Von Holy, A. 2006. What food safety professionals should know about bacterial biofilms. *Br. Food J.* **108**: 27–37. doi:10.1108/00070700610637616.
- Loferer-Krössbacher, M., Klima, J., and Psenner, R. 1998. Determination of bacterial cell dry mass by transmission electron microscopy and densitometric image analysis. *Appl. Environ. Microbiol.* **64**: 688–694. PMID:9464409.
- López-Diez, E.C., Winder, C.L., Ashton, L., Currie, F., and Goodacre, R. 2005. Monitoring the mode of action of antibiotics using Raman Spectroscopy: Investigating subinhibitory effects of amikacin on *Pseudomonas aeruginosa*. *Anal. Chem.* **77**: 2901–2906. doi:10.1021/ac048147m. PMID:15859609.
- Majtán, J., Majtánová, Ľ., Xu, M., and Majtán, V. 2008. In vitro effect of subinhibitory concentrations of antibiotics on biofilm formation by clinical strains of *Salmonella enterica* serovar Typhimurium isolated in Slovakia. *J. Appl. Microbiol.* **104**: 1294–1301. doi:10.1111/j.1365-2672.2007.03653.x. PMID:18028358.
- Mangalappalli-Illathu, A.K., and Korber, D.R. 2006. Adaptive resistance and differential protein expression of *Salmonella enterica* serovar Enteritidis biofilms exposed to benzalkonium chloride. *Antimicrob. Agents Chemother.* **50**: 3588–3596. doi:10.1128/AAC.00573-06. PMID:16940079.
- Mangalappalli-Illathu, A.K., Lawrence, J.R., Swerhone, G.D.W., and Korber, D.R. 2008. Architectural adaptation and protein expression patterns of *Salmonella enterica* serovar Enteritidis biofilms under laminar flow conditions. *Int. J. Food Microbiol.* **123**: 109–120. doi:10.1016/j.ijfoodmicro.2007.12.021. PMID:18261816.
- McLandsborough, L., Rodriguez, A., Perez-Conesa, D., and Weiss, J. 2006. Biofilms: at the interface between biophysics and microbiology. *Food Biophys.* **1**: 94–114. doi:10.1007/s11483-005-9004-x.
- McMurry, L.M., Oethinger, M., and Levy, S.B. 1998. Triclosan targets lipid synthesis. *Nature*, **394**: 531–532. doi:10.1038/28970. PMID:9707111.
- Méchin, L., Dubois-Brissonnet, F., Heyd, B., and Leveau, J.Y. 1999. Adaptation of *Pseudomonas aeruginosa* ATCC 15442 to didecylmethylammonium bromide induces changes in membrane fatty acid composition and resistance of cells. *J. Appl. Microbiol.* **86**: 859–866. doi:10.1046/j.1365-2672.1999.00770.x. PMID:10347880.
- Mooney, L.D. 2006. Triclosan's effects on natural aquatic biofilms, and micro-niche biofilm formation. M.Sc. thesis, Department of Applied Microbiology and Food Science, University of Saskatchewan, Saskatoon, Sask.
- Neu, T.R., and Lawrence, J.R. 2005. One-photon versus two-photon laser scanning microscopy and digital image analysis of microbial biofilms. *In* *Microbial imaging. Methods in microbiology*. Vol. 34. Edited by T. Savidge and C. Pothulakis. Chap. 4. pp. 89–136.
- Neu, T., Swerhone, G.D., and Lawrence, J.R. 2001. Assessment of lectin-binding-analysis for in situ detection of glycoconjugates in biofilm systems. *Microbiology*, **147**: 299–313. PMID:11158347.
- Okamoto, A.C., Gaetti-Jardim, E., Jr., Arana-Chavez, V.E., and Avila-Campos, M.J. 2002. Influence of subinhibitory concentrations of antimicrobials on hydrophobicity, adherence and ultrastructure of *Fusobacterium nucleatum*. *Braz. J. Microbiol.* **33**: 178–184. doi:10.1590/S1517-83822002000200017.
- Okuyama, H., Itoh, H., Fukunaga, N., and Sasaki, S. 1984. Separation and properties of the inner and outer membranes of a psychrophilic bacterium, *Vibrio* sp. strain ABE-I. *Plant Cell Physiol.* **25**: 1255–1264.
- Ouattara, B., Simard, R.E., Holley, R.A., Piette, G.J.P., and Bégin, A. 1997. Inhibitory effect of organic acids upon meat spoilage Bacteria. *J. Food Prot.* **60**: 246–253.
- Prakash, B., Veeregowda, B.M., and Krishnappa, G. 2003. Biofilms: A survival strategy of bacteria. *Curr. Sci.* **85**: 1299–1307.
- Rowan, N.J. 1999. Evidence that inimical food-preservation barriers alter microbial resistance, cell morphology and virulence. *Trends Food Sci. Technol.* **10**: 261–270. doi:10.1016/S0924-2244(99)00060-6.
- Sampathkumar, B., Khachatourians, G.G., and Korber, D.R. 2003. High pH during trisodium phosphate treatment causes membrane damage and destruction of *Salmonella enterica* serovar Enteritidis. *Appl. Environ. Microbiol.* **69**: 122–129. doi:10.1128/AEM.69.1.122-129.2003. PMID:12513986.
- Steinberger, R.E., Allen, A.R., Hansma, H.G., and Holden, P.A. 2002. Elongation correlates with nutrient deprivation in *Pseudomonas aeruginosa*–unsaturated biofilms. *Microb. Ecol.* **43**: 416–423. doi:10.1007/s00248-001-1063-z. PMID:12043001.
- Stewart-Ornstein, J., Hitchcock, A.P., Hernández-Cruz, D., Henklein, P., Overhage, J., Hilpert, K., et al. 2007. Using intrinsic X-ray absorption spectral differences to identify and map peptides and proteins. *J. Phys. Chem. B*, **111**: 7691–7699. doi:10.1021/jp0720993. PMID:17559260.
- Suci, P.A., Mittelman, M.W., Yu, F.P., and Geesey, G.G. 1994. Investigation of ciprofloxacin penetration into *Pseudomonas aeruginosa* biofilms. *Antimicrob. Agents Chemother.* **38**: 2125–2133. PMID:7811031.
- Tattawasart, U., Hann, A.C., Maillard, J.Y., Furr, J.R., and Russell, A.D. 2000a. Cytological changes in chlorhexidine resistant isolates of *Pseudomonas stutzeri*. *J. Antimicrob. Chemother.* **45**: 145–152. doi:10.1093/jac/45.2.145. PMID:10660495.
- Tattawasart, U., Maillard, J.Y., Furr, J.R., and Russell, A.D. 2000b. Outer membrane changes in *Pseudomonas stutzeri* resistant to chlorhexidine acetate and cetylpyridinium chloride. *Int. J. Antimicrob. Agents*, **16**: 233–238. doi:10.1016/S0924-8579(00)00206-5. PMID:11091041.
- van Overbeek, L.S., Eberl, L., Givskov, M., Molin, S., and van Elsas, J.D. 1995. Survival of, and induced stress resistance in, carbon-starved *Pseudomonas fluorescens* cells residing in soil. *Appl. Environ. Microbiol.* **61**: 4202–4208. PMID:8534087.
- Warwick, T., Ade, H., Kilcoyne, A.L.D., Kritscher, M., Tyliczcak, T., Fakra, S., et al. 2002. A new bend magnet beam line for scanning transmission X-ray microscopy at the Advanced Light Source. *J. Synchrotron Radiat.* **9**: 254–257. doi:10.1107/S0909049502005502. PMID:12091736.
- Watkin, E.L.J., O'Hara, G.W., and Glenn, A.R. 2003. Physiological responses to acid stress of an acid-soil tolerant and an acid-soil sensitive strain of *Rhizobium leguminosarum* biovar *trifolii*. *Soil Biol. Biochem.* **35**: 621–624. doi:10.1016/S0038-0717(03)00012-9.
- Wojnicz, D., and Jankowski, S. 2007. Effects of subinhibitory concentrations of amikacin and ciprofloxacin on the hydrophobicity and adherence to epithelial cells of uropathogenic *Escherichia coli* strains. *Int. J. Antimicrob. Agents*, **29**: 700–704. doi:10.1016/j.ijantimicag.2007.01.007. PMID:17382520.
- Wolfaardt, G.M., Lawrence, J.R., Robarts, R.D., Caldwell, S.J., and Caldwell, D.E. 1994a. Multicellular organization in a degradative biofilm community. *Appl. Environ. Microbiol.* **60**: 434–446. PMID:16349173.
- Wolfaardt, G.M., Lawrence, J.R., Robarts, R.D., and Caldwell, D.E. 1994b. The role of interactions, sessile growth, and nutrient amendments on the degradative efficiency of a microbial consortium. *Can. J. Microbiol.* **40**: 331–340. doi:10.1139/m94-055. PMID:8069778.
- Wolfaardt, G.M., Lawrence, J.R., and Korber, D.R. 1999. Function of EPS in microbial biofilms. *In* *Microbial extracellular sub-*

- stances. *Edited by* J. Wingender, T.R. Neu, and H.-C. Flemming. Springer-Verlag, Berlin. Chap. 10. pp. 171–200.
- Young, K.D. 2003. Bacterial shape. *Mol. Microbiol.* **49**: 571–580. doi:10.1046/j.1365-2958.2003.03607.x. PMID:12914007.
- Young, K.D. 2006. The selective value of bacterial shape. 2006. *Microbiol. Mol. Biol. Rev.* **70**: 660–703. doi:10.1128/MMBR.00001-06. PMID:16959965.